# Lawrence Berkeley National Laboratory
## Recent Work

**Title**

DECAY MEASUREMENTS IN EMULSION OF PARTICLES ON NEGATIVE STRANGENESS

**Permalink**

https://escholarship.org/uc/item/9t87634d

**Authors**

Barkas, Walter H.
Dyer, John N.
Mason, Conrad J.
et al.

**Publication Date**

1961-05-02

# UNIVERSITY OF CALIFORNIA

## Ernest O. Lawrence

## Radiation

## Laboratory

BERKELEY, CALIFORNIA

## DISCLAIMER

# UNIVERSITY OF CALIFORNIA

Lawrence Radiation Laboratory
Berkeley, California

## DECAY MEASUREMENTS IN EMULSION
## ON PARTICLES OF NEGATIVE STRANGENESS

Walter H. Barkas, John N. Dyer, Conrad J. Mason,
Norris A. Nickols, and Frances M. Smith

May 2, 1961

# DECAY MEASUREMENTS IN EMULSION
## ON PARTICLES OF NEGATIVE STRANGENESS

Walter H. Barkas, John N. Dyer, Conrad J. Mason,
Norris A. Nickols, and Frances M. Smith

Lawrence Radiation Laboratory
University of California
Berkeley, California

May 2, 1961

## ABSTRACT

We report the results of our program of measurement on decay processes of $K^-$ mesons, $\Lambda$ hyperons, and charged $\Sigma$ hyperons. Experimental and analytical techniques are outlined. The abundances of the $K^-$-meson decay modes were found to be $K_{\mu 2}^-$ (56.5 ± 7.3%), $K_{\mu 3}^-$ (9.5 ± 4.3%), $K_{\pi 2}^-$ (26.3 ± 6.6%), $\tau^-$ (0 + 2.1%), $\tau'^-$ (2.8 ± 2.4%), and $K_{e3}^-$ (4.9 ± 3.2%). The mean life of the $K^-$ meson is $1.25^{+0.22}_{-0.17} \times 10^{-8}$ sec. Measurements on 116 $\Lambda$-hyperon decay events in two emulsion stacks determined the $\Lambda$-hyperon mass to be 1115.36 ± 0.14 Mev, using 938.213 Mev and 139.59 ± 0.05 Mev for the proton and pion masses. The Q value derived from these masses is 37.56 ± 0.13 Mev. In an analysis of about 200 hyperfragment decays, no leptonic modes of bound $\Lambda$ hyperons were observed. Some 390 charged $\Sigma$-hyperon decay events were studied. The proton range from the mode $\Sigma^+ \rightarrow p + \pi^0$ is 1677.5 ± 3.2 μ, corresponding to a momentum of 189.01 ± 0.20 Mev/c The mass of the $\Sigma^+$ hyperon from this measurement is 1189.33 ± 0.22 Mev. From the decay mode $\Sigma^+ \rightarrow n + \pi + \pi^+$, the $\pi^+$ range is 92.48 ± 0.49 mm, corresponding to a momentum of 184.44 ± 0.05 Mev/c, and a $\Sigma^+$ mass of 1188.75 ± 0.54 Mev. If the mass of

the neutral particle in the proton decay mode is considered unknown, these measurements imply a mass of $134.0 \pm 1.0$ Mev for it, consistent with the $\pi^0$ mass of $135.0 \pm 0.05$ Mev. Studies of the hyperon mean lives gave, for the $\Sigma^+$ hyperon, $0.82^{+0.10}_{-0.08} \times 10^{-10}$ sec, and for the $\Sigma^-$ hyperon, $1.75^{+0.39}_{-0.30} \times 10^{-10}$ sec. Reasons for experimental biases that have affected some emulsion measurements are discussed. The branching ratio $\Sigma^+ \to (p + \pi^0)$ / (all $\Sigma^+$ decay) was found to be $0.50 \pm 0.03$. No example of the decay mode $\Sigma^+ \to p + \gamma$ was found in a sample of 95 $\Sigma^+ \to p$ decay events. No $\Sigma^+$ leptonic decay events were observed among 129 $\pi^+$ decays, nor any $\Sigma^-$ leptonic modes among 67 $\pi^-$ events. No up-down decay asymmetry was detected in any mode for charged hyperons emitted from complex nuclei in association with a charged pion.

# DECAY MEASUREMENTS IN EMULSION
## ON PARTICLES OF NEGATIVE STRANGENESS[*]

Walter H. Barkas, John N. Dyer,[†] Conrad J. Mason,[‡]
Norris A. Nickols, and Frances M. Smith

Lawrence Radiation Laboratory
University of California
Berkeley, California

May 2, 1961

## I.  INTRODUCTION

During the past few years we have exposed several large emulsion stacks to $K^-$ mesons.

Those $K^-$ mesons that do not decay interact with nucleons, producing either $\Sigma$ or $\Lambda$ hyperons. The hyperons, in turn, decay or interact. Much valuable information about K mesons and hyperons can be gained by observing their decay behavior and their interactions.

This paper is mainly devoted to the analysis of measurements we have taken on decay events of these three types of particles.

The studies began with the creation of the first copious beam of negative K mesons.[1] Additional data were collected by using several other beams, to which a number of stacks were exposed.[2,3] For the analysis, automatic equipment and data-processing systems were developed.[4-7] Also during this period, the scanners—who deserve much credit—developed skills and techniques that were essential for the more difficult parts of the work.

The data were obtained from the four emulsion stacks listed in Table I. Information regarding the beam to which each was exposed is included in the table.

Table I.  Emulsion stacks used for strange-particle decay measurements

| Stack | Emulsion type | K-meson momentum (Mev/c) | Stack dimensions (in.) |
|---|---|---|---|
| 1U | G.5 600 μ | 300 | 120 pellicles 3×6 |
| 2B | G.5 600 μ | 300 | 240 pellicles 9×12 |
| 2D | K.5 600 μ | 430 | 108 pellicles 3×6 |
| A | K.5 600 μ | 430 | 216 pellicles 6×9 |

A feature of the 1U and 2B stacks was that they were exposed to a K-meson beam that had been deflected through 180 deg. The stacks were placed along the 180-deg focal line. Under these conditions, the mesons entering the stack at a given point all had nearly the same momentum. Mesons of different momenta, of course, had different radii of curvature, but in a pellicle they came to rest along a line with little straggling. This fact was utilized to establish most accurately the velocity of mesons that decayed in flight, the residual range being the most reliable means for estimating it.

## II.  MEASUREMENTS

### A.  Density and Thickness

The density of the emulsion in each stack was determined by weighing

pellicles—or, in some cases, pieces cut from pellicles—in air and in carbon

tetrachloride.  Original thicknesses were then calculated from the density,

weight, and area of each pellicle.  These methods are described in more

detail in Refs. 4, 5, 8, and 9.

### B.  Ionization

A special microscope with a motor-driven stage and an electronic

data tabulator was built to aid the ionization measurements in this work.

With one traversal of the track, this device tabulates the blob density,

density of gaps greater than a preset length, and the lacunarity (or linear

transparency).  This device is described more fully in Ref. 8.  Decay secondaries

that left the stack or interacted in flight were blob-counted for at least 1000 counts

near their termination in order to determine their momenta at the decay point.

A calibration of blob density as a function of residual range was made for

tracks of stopping $\pi$ mesons.  The minimum blob density in each pellicle used

for counting was established from secondaries of the identified two-body decays

near their decay point.  A dip-angle correction was applied to all blob counts.

For particles with velocity parameter $\beta$ less than 0.4, lacunarity was

chosen as the measure of ionization.  Nearly all the charged hyperons that decayed in

flight, and some of the decaying $K^-$ mesons, fell within this velocity region.

Calibration curves were established in the A and 2B stacks by using K mesons,

protons, and hyperons of known velocity.  Appropriate corrections for dipping

tracks were derived and verified.  The effects of nonuniformity of development

were eliminated by calibration and by counting track segments through the whole

pellicle thickness.

## C. Range

All range measurements on tracks whose ranges exceeded 1 mm

were performed on an automated microscope specifically designed to facilitate

such measurements in large emulsion pellicles. [4,6] The ranges were calculated

from coordinates of points on the tracks that were read out on IBM cards.

Periodicity in microscope lead screws does not permit precise measurements

of ranges less than 1 mm—a calibrated reticle was employed as a substitute.

The method of range rectification was based upon the conventions adopted

by Barkas et al. to establish the range-energy relation in emulsion. [9]

Before any measurements were taken in a particular pellicle, its

thickness was determined at a standard reference point. Comparison of

this value with the original thickness allows an evaluation of the shrinkage

factor to be applied in the subsequent range calculations.

Since the range-energy relation was established for emulsion with the

standard density 3.815 g/cc, corrections were applied to ranges measured in

emulsion of a different density.

The statistical errors present in the range measurements are range

straggling and measurement error. The magnitude of the former is well known

for emulsion and has been evaluated as a function of velocity. [10,11] Measurement

errors are described in subsequent sections of this paper.

Various systematic errors are inherent in the range calculations, primary

among these being the errors in measured emulsion density and in shrinkage

factors. The uncertainty in density, though small ($\pm 0.1\%$), is reflected almost

directly into a range uncertainty of the same order of magnitude. An un-

certainty in the shrinkage factor produces a range error difficult to evaluate

generally because the magnitude of the error is dependent upon the geometry of the track. On the assumption that the error in shrinkage factor was equal to its experimental error of $\pm 1\%$, the range error was calculated explicitly for each track—no general evaluation was attempted.

## D. Angles

The space angle between the directions of two tracks was computed from the projected angle between them, and from their dip angles. Statistical errors in projected angle measurements arise from multiple scattering of the particles, from observer errors, and from granularity. To minimize the error caused by small-angle scatterings near the origin of the event, the shortest length of track consistent with obtaining a reliable measurement was used, in lieu of a rigid convention. Using two independent observations of each event, in $\Lambda$-hyperon decay, for example, the projected angle was measured with an observer standard deviation of 0.2 degree. The statistical error on the dip angle arises chiefly from observer errors and must be estimated for each case since it varies with dip angle. The only systematic error in the space angle originates in the shrinkage-factor error of $\pm 1\%$.

## III.   K⁻-MESON DECAY

A large stack, the 2B stack, was exposed for the study of K⁻-meson decay.   Along-the-track scanning provided a sample of decay events with minimum bias.   Tracks found at the entrance edge of the stack, with the proper ionization and direction for a K⁻ meson were followed to their termination.

Of the 2582 certified K⁻ mesons followed in the 2B stack, 2156 came to rest and interacted, and 426 made stars in flight.  Of the in-flight events, 48 had one lightly ionizing secondary with no blob or Auger electron, and were classed as decay-like events;  38 had no visible secondary, blob, or electron, and were called disappearances in flight.   Each of the decay-like events whose secondary could be a pion is a possible K⁻-meson interaction in flight, and each of the disappearances in flight is a possible decaylike event with an undiscovered near-minimum secondary.

### A.   Decay Modes

Because of the momentum gradient and low dispersion of the beam, there is a well-defined mean stopping line for K⁻ mesons in the 2B stack. This line was determined graphically by plotting the interaction point of each stopping K⁻ meson on a graph-paper representation of the grid, ten times actual size.   These points lie along a straight line, as shown in Fig. 1.   The lines on either side of the mean stopping line are standard-deviation lines which enclose 68% of the interaction points.   The residual range of a decaying K meson is then the distance along the beam direction from the decay point to the mean stopping line, with a standard deviation given by the distance from the mean stopping line to the standard deviation line at that point.   This determines the momenta (with standard deviations less than 10%) for K mesons with residual ranges greater than 5 mm.   Ionization measurements were used to determine the residual ranges of mesons that decayed within 5 mm of the mean stopping line.

The kinematics of the decay of a charged particle into one charged and one neutral particle are described by the relativistic invariant

$$E_1 E_2 - P_1 P_2 \cos \theta = C, \quad C = 1/2 \, (M_1^2 + M_2^2 - M_n^2) \,,$$

where the subscripts 1, 2, and n refer to the primary, the charged secondary, and the neutral particles, respectively; $\theta$ is the laboratory-system angle between their directions; E is the total energy of a particle; P is its momentum; and C is the given function of the masses of the three particles.

A program was written for the IBM 650 computer which determines, from the angle measurements, the space angle and its total error. From this space angle, the K-meson momentum, and the error on the K-meson momentum, the computer determines secondary momenta for given decay modes, together with their total errors. For three-body modes it computes maximum secondary momenta. The modes consistent with each decay-like event were found by comparing these secondary momenta with the momentum computed from the ionization or range measurements on the secondary, for each possible particle identity. Only the modes established for $K^+$ mesons were considered. [12, 13]

Nineteen of the secondaries were identified by terminal behavior or scatterings in flight. Four of the secondaries left the stack a short distance from the decay point—with ionization near the plateau—and, therefore, could have been electrons. All of these were too steep for multiple-scattering measurements. Many of the events are consistent with more than one mode, and each event whose secondary could be a pion is possibly a nuclear interaction.

To determine the distribution of the decaylike events among the modes considered—$K_{\mu 2}$, $K_{\pi 2}$, $K_{\mu 3}$, $K_{e 3}$, $\tau'$, and nuclear interaction—we derived a probability matrix P, of which an element $P_{ij}$ gives the probability that

the ith event belongs to the jth mode. Then $\Sigma_i P_{ij}$ is the population of the jth mode. The $P_{ij}$ were determined as follows: Momentum probability distributions, $p_{ij}(p)$, were calculated for each possible identity of the ith secondary, and, therefore, mode of the event,-from the ionization or range measurements made on each secondary and from their associated errors. The K-meson momentum, the space angle, and their associated errors provide a second set of probability functions, $F_{ij}(p)$, for the secondary momentum of the ith event, assuming each possible mode. For events whose secondaries are identified, there are at most three possible modes, and the $p_{ij}$ for these are equal. In this case

$$P_{ij} = \frac{\int p_{ij}\, F_{ij}\, dp}{\Sigma_j \int p_{ij}\, F_{ij}\, dp}\ ,$$

and the $P_{ij}$ for modes with other secondary particles are set equal to zero.

Secondaries that were not identified left the stack after traveling a distance $x_i$ without undergoing an identifying interaction or decay. The probability that a pion will survive a distance greater than $x$ without suffering an identifying interaction or decay is $\exp(-x/\lambda_\pi)$, where $\lambda_\pi \approx 30$ cm is the pion mean free path in emulsion for interaction or decay. Since the mean free path in emulsion for a muon to scatter more than 7 deg is 18 m,[14] this possibility is negligible; but $\lambda_\mu \approx 18$ m may be retained as the muon mean free path for interaction. Finally, an electron is recognized by its characteristic rate of radiative energy loss. The radiation length in emulsion, $\lambda_e = 3.0$ cm, was taken here as a mean free path for an identifying energy loss by an electron. Thus we have characteristic lengths, $\lambda_j$, for each mode. With this information the complete expression for the $P_{ij}$ is

$$P_{ij} = \frac{\exp(-x_i/\lambda_j) \int P_{ij} \, F_{ij} \, dp}{\Sigma_i \, \exp(-x_i/\lambda_j) \int P_{ij} \, F_{ij} \, dp} \, .$$

These $P_{ij}$ are presented in Table II.

The integrals in the expression for the $P_{ij}$ were evaluated graphically, with the $F_{ij}$ for two-body decays plotted as normal probability curves and those of the three-body decays approximated by triangles with maximum probability at $2/3$ the maximum momentum. The spectrum $F_{int}$, used for the $\pi^-$ from nuclear interactions in flight, is that shown in Fig. 2. Eisenberg et al. have calculated the spectrum of $\pi^-$ expected from the in-flight interactions,[15]

$$K^- + n \rightarrow \pi^- + \Lambda \, ,$$
$$\rightarrow \pi^- + \Sigma^0 \, ,$$

for pion energies up to 100 Mev and for $K^-$-meson energies from 5 to 150 Mev, taking into account scattering of the pion in the nucleus. These curves are roughly the same and agree with the spectrum of pions observed by Eisenberg et al. The curve used here, Fig. 2 is their curve for $\Lambda$ $\pi$-production plotted against momentum, and is made to decrease linearly to zero at 395 Mev/c, the maximum pion momentum obtainable at the $K^-$-meson energies under consideration.

This spectrum (Fig. 2) was calculated for all interactions in flight, and may not be correct for decaylike interactions, as it might be expected that the pions from them would have scattered less within the nucleus and would leave the nucleus with greater energy. However, Eisenberg et al. find that the pions from events in flight with no stable prongs seem to have the same spectrum as those from all events in flight, which would indicate that they do scatter as much.[15] The decaylike interactions in this study are also consistent with this assumption, although not enough data have been obtained in either study to determine the pion

Table II.   Probability distribution of decaylike events

| Event | $K_{\mu 2}$ | $K_{\mu 3}$ | $K_{\pi 2}$ | $K_{\pi 3}$ | $K_{e3}$ | Interaction |
|---|---|---|---|---|---|---|
| 1 | | | | | | 1.00 |
| 2 | | | | | | 1.00 |
| 3 | | | | | | 1.00 |
| 4 | | | | | | 1.00 |
| 5 | | | 0.98 | | | 0.02 |
| 6 | | | | | | 1.00 |
| 7 | | | | 0.71 | | 0.29 |
| 8 | | | | | | 1.00 |
| 9 | | | 0.83 | | | 0.17 |
| 10 | | | | | | 1.00 |
| 11 | | | | 0.62 | | 0.38 |
| 12 | | | 0.91 | | | 0.09 |
| 13 | | | 0.93 | | | 0.07 |
| 14 | | | | | | 1.00 |
| 15 | | | 0.98 | | | 0.02 |
| 16 | | | 0.84 | | | 0.16 |
| 17 | | | 0.89 | | | 0.11 |
| 18 | | | 0.86 | | | 0.14 |
| 19 | | | | | 1.00 | |
| 20 | 1.00 | | | | | |
| 21 | 0.91 | 0.05 | | | | 0.04 |
| 22 | 0.99 | | | | | 0.01 |
| 23 | 0.75 | | | | | 0.25 |
| 24 | 0.99 | | | | | 0.01 |
| 25 | 0.98 | 0.02 | | | | |
| 26 | 0.93 | 0.06 | | | | 0.01 |
| 27 | 0.99 | 0.01 | | | | |
| 28 | | 0.88 | | | | 0.12 |
| 29 | 0.60 | 0.23 | | | | 0.17 |
| 30 | 0.99 | | | | | 0.01 |
| 31 | 0.89 | | | | | 0.11 |
| 32 | 0.74 | 0.10 | 0.13 | | | 0.03 |
| 33 | | 0.47 | 0.45 | | | 0.08 |
| 34 | 0.96 | | | | | 0.04 |
| 35 | 0.65 | -.10 | 0.17 | | | 0.08 |
| 36 | 0.14 | 0.52 | 0.17 | | | 0.17 |
| 37 | 0.88 | 0.01 | | | 0.07 | 0.04 |
| 38 | 0.81 | 0.12 | | | | 0.07 |
| 39 | 0.93 | | | | | 0.07 |
| 40 | 0.78 | | | | | 0.22 |
| 41 | | 0.19 | 0.69 | | | 0.12 |
| 42 | 0.81 | | | | 0.14 | 0.05 |
| 43 | 0.66 | 0.08 | 0.06 | | 0.13 | 0.07 |
| 44 | 0.60 | 0.17 | 0.04 | | | 0.19 |
| 45 | 0.85 | 0.05 | 0.01 | | | 0.09 |
| 46 | | 0.34 | 0.49 | | | 0.17 |
| 47 | | | | | | 1.00 |
| 48 | 0.57 | | | | 0.32 | 0.11 |

spectrum of decaylike interactions. In order that the effect of this spectrum on the final results might be seen, the $P_{ij}$ were determined for an extreme case—a uniform spectrum from 100 to 400 Mev/c. This yielded a total of 17.53 interactions among the 48 decaylike events, compared with 12.78 for the spectrum used. Eisenberg et al. have analyzed $K^-$-meson—nuclear interactions in flight which have a blob and one pion secondary, and find that 70% do not fit the kinematics of either of the two-body decay modes.[16] Nine of the decaylike events in our study were not consistent with any mode, from which we would predict a total of 12.9 decaylike interactions if the ratios are the same for events with and without blobs.

The decaylike events are not an unbiased sample, because the secondaries missed are most probably those of the more lightly ionizing two-body modes. The efficiency with which the scanners detected the electrons from muon decays was determined previously to be higher than 95% in pellicles with a minimum blob density near that of the highest in the 2B stack (19 blobs per 100 μ). However, three factors act to lessen the efficiency in finding the secondaries from decaylike events: (a) the scanner knows there is a secondary from the muon decay, but the K meson in flight may or may not have a secondary, (b) the decay point of the muon is well defined, whereas that of the K meson in flight may be several microns from the last blob, and (c) the electron from muon decay is at plateau ionization, which is approximately 15% above minimum.

One estimate of a lower limit to the number of missed decay secondaries may be made from the angular distribution of those detected. Figure 3 shows the distribution of the cosine of the angle between the K meson and the secondary in the center-of-mass system for all the probable two-body decays. These,

of course, would be expected to be isotropic, and decay secondaries missed would most probably be those of $K_{\mu 2}$ or $K_{\pi 2}$, because they contribute the majority of decays and their secondaries are lower in ionization. Eight decays added in the region $-0.5 < \cos\theta < 0$ would make this distribution consistent with uniformity. The secondaries in the region $-0.5 < \cos\theta < 0.5$ are those most likely to be missed because those with $\cos\theta$ less than $-0.5$ will be emitted more slowly in the lab system and hence have a higher grain density, whereas those with $\cos\theta > 0.5$ will tend to be flat.

Figure 4 shows the dip-angle distribution of those secondaries emitted with a c.m. angle between -60 deg and + 60 deg. Again, within statistics, we would expect an even distribution from -90 to + 90 deg. Although there are fewer events in this group, a definite bias for detecting secondaries with dip angles between +30 and -30 deg is evident. Here too, approximately eight additional events with dip angles steeper than 30 deg would be required for axial symmetry. As mentioned before, these estimates would be lower limits to the number of missing decay secondaries, as they are made with the assumption of 100% efficiency in detecting secondaries emitted with a c.m. angle greater than 120 deg or less than 60 deg.

An estimate of an upper limit to this number may be made as follows. Thirteen decaylike nuclear interactions were found which presumably represent the reactions

$$K^- + n \rightarrow Y^0 + \pi^- .$$
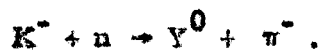
Because there are 1.24 times as many neutrons as bound protons in emulsion, we would expect 11 true disappearances in flight from the reactions

$$K^- + p_{bound} \rightarrow Y^0 + \pi^0 .$$

From the 81 m of $K^-$-meson track followed, we would expect two interactions on free hydrogen of the type

$$K^- + p \to Y^0 + \pi^0 ,$$

and one charge-exchange scattering. This same ratio among the "clean" interactions with bound protons would predict five true disappearances from charge-exchange scatterings on bound protons. This predicts a total of 19 true disappearances or 19 undetected secondaries. Of the decaylike events with secondaries of ionization less than that of a pion with a 10-cm range, 20% are nuclear interactions. This same ratio among the undetected secondaries would leave a total of 15 undetected decay secondaries.

A third estimate (which is probably not as reliable) can be made by comparing the precentage of clean zero-prong interactions at rest with the percentage for in-flight interactions. This ratio is $146/2156 = 0.068$, which would predict 25 disappearances in flight and 13 undetected secondaries if these ratios could be expected to be the same. The first two estimates seem much more reliable, however, and their average, $11.5 \pm 3.4$, will be used as the best estimate of the number of undetected decay secondaries. These secondaries are divided among the decay modes in the same ratio as the analyzed decaylike events with ionization less than that of a "10-cm pion:" 60.7% $K_{\mu 2}$, 8.9% $K_{\mu 3}$, 24.8% $K_{\pi 2}$, and 5.6% $K_{e3}$. This gives the following for the total population of each mode.

| Mode | Decaylike events | Undetected secondaries | Total |
|---|---|---|---|
| $K_{\mu 2}$ | 19.40 | 6.98 | 26.4±5.1 |
| $K_{\mu 3}$ | 3.40 | 1.02 | 4.4±2.1 |
| $K_{\pi 2}$ | 9.43 | 2.85 | 12.3±3.5 |
| $K_{\pi 3}$ | 1.33 | 0.00 | 1.3±1.2 |
| $K_{e 3}$ | 1.66 | 0.64 | 2.3±1.5 |
| All | 35.22 | 11.50 | 46.7±6.8 |

No $\tau'$ mesons were found in this study, although they have of course been seen by others,[10,17] and are the most easily detected decay mode. The likelihood of there being n events when none are observed is given by $e^{-n}$, which gives a maximum likelihood of zero with an rms spread of 1.0. We have, finally, the percent abundances:

| | |
|---|---|
| $K_{\mu 2}^{-}$ | 56.5±7.3 |
| $K_{\mu 3}^{-}$ | 9.5±4.3 |
| $K_{\pi 2}^{-}$ | 26.3±6.6 |
| $\tau'^{-}$ | 2.8±2.4 |
| $K_{e 3}^{-}$ | 4.9±3.2 |
| $\tau^{-}$ | 0.0+2.1 |

Only the statistical errors have been included.

## B.  The Lifetime Calculation

The proper time during which a $K^-$ meson could have decayed and could have been detected was derived from its observed range by using the tables of Barkas and Young.[18]  For the in-flight events, the residual proper time to the mean stopping line at the star was subtracted from that at the entrance edge. From the 2156 $K^-$ mesons that came to rest, the total proper time was $5.91 \times 10^{-7}$ sec, and from the 426 in-flight events the total was $4.96 \times 10^{-8}$ sec, making a grand total of $6.41 \times 10^{-7}$ sec.  For the lifetime calculation we eliminate from consideration the segment of track at the end of its range in which a $K^-$ meson, had it decayed, might have been considered to be at rest. This segment was estimated to be 0.3 mm, and none of the decaylike events was in this range.  We also eliminate from consideration the first mm of track from the pickup line, since events in this region were not recorded in the initial scanning and could not be distinguished from neutron-induced stars with outgoing prongs.  These corrections leave a total proper time of $6.06 \times 10^{-7}$ sec (46.7 ±6.8 decays), which yields, for the $K^-$-meson mean lifetime, $1.30^{+0.22}_{-0.17} \times 10^{-8}$ sec.

Because secondaries from events near the top and bottom surfaces are more likely to escape detection, the lifetime calculated with the top and bottom surfaces of each pellicle excluded is probably less subject to systematic error.  Only two of the decaylike events lie within 30 $\mu$ of either surface, whereas we would expect five from a uniform distribution.  Three of the disappearances in flight lie in this region.  Excluding the top and bottom 30 $\mu$ of unprocessed emulsion leaves a total proper time of $5.49 \times 10^{-7}$ sec, 33.5 decays from the decaylike events, and 10.5 decays with undetected secondaries, or a total of 44.0 ±6.6 decays.  This yields $1.25^{+0.22}_{-0.17} \times 10^{-8}$ sec for the $K^-$-meson mean lifetime.

The lifetime value is in excellent agreement with that of the $K^+$ meson, $1.224\pm0.013\times10^{-8}$ sec[19] (see also Ref. 20). The relative abundances are in reasonably good agreement with the values determined by Birge et al.[12] and by Alexander, Johnson, and O'Ceallaigh,[13] except for (a) that of the $\tau^-$ mode, which is considerably lower than the $\tau^+$ abundance quoted by either group, and (b) the $K_{\mu3}^-$ abundance, which is higher than either $K_{\mu3}^+$ abundance but within one standard deviation of that quoted by Alexander, Johnson, and O'Ceallaigh.

## C. Interpretation

PCT invariance requires that the particle and antiparticle lifetimes be identical,[21] but does not by itself require equality of the branching ratios into charge-conjugate decay channels. However, under any of the following conditions the partial lifetimes of corresponding modes will be identical: (a) T, or C, is separately conserved, (b) there are no final-state interactions leading to transitions between different decay products,[21] and (c) the decay is by $\Delta I = 1/2$.[22] Luders and Zumino have shown that the branching ratios for the two- and three-pion modes must be the same for spin-zero $K^+$ and $K^-$ mesons.[21] Neglecting weak interactions, the charge-conjugate leptonic-mode abundances must be identical, since there are no final-state interactions. The distributions of the three-pion mode into $\tau$ and $\tau'$ may differ,[21] but not if the decay is by $\Delta I = 1/2$.[22]

## IV. Λ-HYPERON DECAY

In both the 2B and 2D stacks, the events corresponding to Λ-hyperon decays were located by area-scanning the region in which the $K^-$ mesons came to rest. Thirty-five two-prong events, characterized by a "clean" origin and secondaries identified as a proton and a $\pi^-$ meson, were found in the volume scanned (160 cm$^3$) in the 2B stack; for the 2D stack, 92 similar events were found in a scanned volume of 50 cm$^3$. The scanning efficiencies for locating Λ-like events are markedly different for the two stacks. Because of the relatively large amount of background present in the 2B stack, the average scanning efficiency is $\approx 15\%$. On the other hand, this figure is $\approx 41\%$ for the 2D stack. Only those Λ-like events whose secondaries came to rest were used in the mass determination. Although it is possible to determine the residual range of a particle that interacts in flight by means of grain-counting techniques, the uncertainty in this quantity is such as to preclude obtaining precise results in a mass determination.

### A. Mass and Q Value

The equations relating the mass and Q value of the Λ hyperon in the decay $\Lambda \rightarrow p + \pi^-$ to the energies of the secondaries and to the space angle between them can be written

$$M_\Lambda = M_p \left\{ 1 + \left( \frac{M_\pi}{M_p} \right) \frac{M_\pi}{M_p} + 2 \left( \gamma_p \gamma_\pi - \sqrt{(\gamma_p^2 - 1)(\gamma_\pi^2 - 1)} \cos \phi \right) \right\}^{1/2} ,$$

(1)

$$Q = M_\Lambda - (M_p + M_\pi) ,$$

(2)

where $M_\Lambda, M_p,$ and $M_\pi$ are the rest masses of the hyperon, proton, and pion, respectively; $\gamma_p$ and $\gamma_\pi$ are the relativistic parameters for the proton and pion; and $\phi$ is the space angle.

By use of Eq. (1) above, the mass and its total statistical error (which results from statistical errors in range and angle measurements) were evaluated for each event.

The weighted means of the mass values, with the computed statistical error of each event used as the weighting factor, were determined for the two stacks; the results are:

2B stack:  $M_\Lambda = 1115.26 \pm 0.11$ Mev (29 events),

2D stack:  $M_\Lambda = 1115.42 \pm 0.08$ Mev (87 events).

The error quoted is the internal standard deviation of the mean.  The mass-value ideogram for the 2B stack is shown in Fig. 5 and that for the 2D stack in Fig. 6.  All events for which mass values differed from the mean by more than 2.5 standard deviations were considered background events.  The 2B and 2D stacks contained six and five such events, respectively—indicated in the ideograms by the shaded areas.

The internal and external errors were in very good agreement for the 2B stack.  For the 2D stack, the internal error was 0.02 Mev greater than the external error;  the discrepancy resulted from a broadening of the distribution because of the statistical fluctuation in the shrinkage factor, an effect not considered in the calculation of the total statistical error associated with each event.  The 2B stack events have secondaries that lie predominantly in the plane of the emulsion, since presence of background hindered the detection of steep secondaries.  Naturally, these "flat" events are less subject to errors in shrinkage factors;  consequently, the aforementioned agreement between internal and external errors for the 2B stack is to be expected if other undetected sources of error are absent.

Systematic errors for the mean values cited previously were evaluated on the following bases: the uncertainty in the mass value of each event arising from a given systematic error was calculated explicitly; the systematic error in the mean value from this source equals the average of these mass uncertainties. The systematic errors include uncertainties in (a) the measured emulsion density, (b) the shrinkage factors, (c) the range-energy relation, and (d) the rest masses of the pion and proton. Table III lists the magnitudes of these errors and, for each stack, the resultant mean errors in the mean masses. The mass uncertainty resulting from the shrinkage-factor uncertainty differs for the two stacks because of the aforementioned difference in the geometries of the events in the stacks.

Prior to calculation of a weighted mean mass for the two stacks, the systematic and statistical errors in mass associated with a stack must be compounded. These systematic errors, which become random in nature when a number of stacks are involved, are (a) the uncertainty in the emulsion density, and (b) the uncertainty in the shrinkage factors. Being now a combination of statistical, density, and shrinkage-factor errors, the total "statistical" uncertainty in the mean mass for the 2B stack remains $\pm 0.11$ Mev, whereas for the 2D stack its value becomes $\pm 0.09$ Mev. For these total errors, a comparison of the mean mass values for the two stacks shows no inconsistency. A $\chi^2$ test indicates that one would expect two measurements to differ by at least this amount 28% of the time. Hence, a weighted mean can be obtained; it is $M_A = 1115.36 \pm 0.07$ Mev, and the Q value derived from this figure is $37.56 \pm 0.07$ Mev.

The systematic errors introduced by uncertainties in the range-energy relation and in the rest masses of the secondaries are combined with the above errors in the weighted mean mass and in the $Q$ value to give the results (for 116 events)

$$M_\Lambda = 1115.36 \pm 0.14 \text{ Mev},$$

$$Q = 37.56 \pm 0.13 \text{ Mev}.$$

The values used for the proton and pion rest masses were $938.213 \pm 0.010$ Mev and $139.59 \pm 0.05$ Mev, respectively. [19]

Most of the above computations were performed on the IBM 650 computer.

Three additional sources of error and their possible effects on the mean mass value must be considered: (a) pion inelastic scattering, (b) distortion of the emulsion, and (c) inner bremsstrahlung in the decay.

With regard to (a), the maximum energy loss that a pion could sustain without detectably altering a mass value would be approximately 2 Mev, because an event was considered background if its measured mass differed from the mean by more than 2.5 standard deviations. The probability of such an energy loss is very small. An undetected scattering, moreover, would have little effect on the mean mass; in fact, an event whose mass value is one standard deviation from the mean changes the 2B mean value by only 0.02 Mev and the 2D mean value by only 0.01 Mev.

The effects of emulsion distortion—which are not systematic in nature — are negligible, as demonstrated by the agreement of the internal and external statistical errors for each stack.

An estimate of the effect of inner bremsstrahlung on the mean mass

can be obtained by utilizing the semiclassical expression for the bremsstrahlung

spectrum applied to the decay pion.[23] As in inelastic pion scattering, the maximum

photon energy must be limited to 2 Mev; a greater energy would require classifi-

cation of the event as background. However, the average photon energy as

calculated from the above spectrum with the imposed cutoff of 2 Mev is

only 0.001 Mev—an amount which is completely negligible.

Table III.  Source and magnitude of systematic error and the
resulting mean errors in mean mass

| Source | Magnitude of error | Uncertainty in mass (Mev) | |
| | | 2B stack | 2D stack |
| --- | --- | --- | --- |
| (a) Emulsion density | ±0.1% | ±0.02 | ±0.01 |
| (b) Shrinkage factors | ±1.0% | ±0.03 | ±0.04 |
| (c) Range-energy relation | ±0.5% | ±0.11 | ±0.11 |
| (d) Rest energies | | | |
| Proton | ±0.01 Mev | ±0.01 | ±0.01 |
| Pion | ±0.05 Mev | ±0.05 | ±0.05 |

## B. Search for Leptonic Decay of Bound Λ

Emulsion is not suitable for studying the neutral decay of Λ hyperons, nor is it well adapted to studying leptonic decay of the free Λ. Such an event probably could not be distinguished from background. The presence of hyperfragments among the star prongs made possible the search for electronic decay of the bound Λ, however. No example of an electronic decay was found in some 200 such events examined.

## V. CHARGED Σ-HYPERON DECAY

Charged Σ hyperons were located by following tracks of greater than twice-minimum ionization, produced by $K^-$ interactions at rest. In the A stack, each track was followed to its termination (interaction, decay, or exit from the stack), regardless of the number of prongs constituting the parent $K^-$ star. In the other stacks, however, only the one- and two-pronged stars were completely analyzed—tracks from larger stars were followed only to the surface of the pellicle in which they originated. The sample of decays is unbiased, then, only for the A stack—the remaining events are biased toward those decays which occurred near the parent star. The lifetime estimates are therefore based upon the decays in the A stack alone.

The decay events are listed in Table IV. The nomenclature here follows the example of Evans et al.[24] Thus, $R\Sigma_p^+$ indicates a decay at rest via the mode $\Sigma^+ \to p + \pi^0$, $F\Sigma_\pi^+$ indicates a decay in flight via the mode $\Sigma^+ \to n + \pi^+$, etc.

Table IV.   Charged $\Sigma$-hyperon decay events

| Stack | $R\Sigma_p^+$ | $F\Sigma_p^+$ | $R\Sigma_\pi^+$ | $F\Sigma_\pi^+$ | $F\Sigma_\pi^-$ | $F\Sigma_\pi^\pm$ | Total |
|-------|------|------|------|------|------|------|-------|
| A | 64 | 43 | 51 | 33 | 26 | 35 | 252 |
| 2B | 16 | 21 | 18 | 10 | 12 | 41 | 118 |
| 1U | 14 | 6 | ---not recorded----------------- | | | | 20 |
| Total | 94 | 70 | 69 | 43 | 38 | 76 | 390 |

The identification of the various decay modes is discussed in the sections which follow.

## A.  Masses and Q Values

The decay at rest of the $\Sigma^+$ hyperon furnishes sufficient information for determining the Q value of the decay and the mass of the hyperon.  To be classed as a decay at rest, an event must satisfy two criteria:

(a)  The hyperon track must appear, by ionization and scattering, to terminate at rest.  Generally, however, a decay in flight cannot be distinguished from a decay at rest by the appearance of the hyperon track unless the residual range at the decay point is greater than about $200\,\mu$.  Therefore, we also require

(b)  the secondary particle must have a range compatible with that expected for a decay at rest.

The range of the charged decay product is the measured quantity used to determine the mass and Q value from the decay.  The energy and momentum of the charged decay product are then determined with the aid of

the range-energy relation. Equal momentum is assigned to the neutral decay product, and the mass and $Q$ value are calculated according to the equations

$$M_{\Sigma^+} = (M_0{}^2 + P^2)^{1/2} + (M^2 + P^2)^{1/2} , \qquad (3)$$

$$Q = M_\Sigma - (M + M_0) , \qquad (4)$$

where $M_0$ is the mass of the neutral product, and $M$ and $P$ are the mass and momentum of the charged product, respectively.

## 1. The Decay Mode $\Sigma^+ \to p + \pi^0$ at Rest

The normalized mean proton range from 80 decays (50 in A stack, 14 in 1U stack, and 16 in 2B stack) is $1677.5 \pm 3.2\,\mu$. The individual ranges are weighted by compounding the effects of 1.4% Bohr range straggle, 1% measurement error, and the shrinkage-factor uncertainty. The last is obtained directly for each track by altering the shrinkage factors—by 2% in the A stack and by 1% in the others—and recalculating the ranges. The measurements were performed on the automated microscope described in Refs. 4 and 6, each proton being measured at least twice. In addition, several protons were also measured with microscope reticles in order to check for systematic errors in the automated microscope for these relatively short ranges. No systematic error was found in this way. Each range is normalized to the equivalent range in emulsion of standard density.

The normalized range distribution for the 80 protons is shown in Fig. 7. The spread of the distribution is $28\mu$ (1.43%)—only slightly larger than the spread predicted by straggling alone. Internal and external estimates of the error on the mean range both yield $\pm 3.2\,\mu$. Using now the range-energy relation, [11] we find that the mean range corresponds to a proton of energy $18.85 \pm 0.04$ Mev. The error here results from the range error and an assumed 0.3% systematic error in the range-energy relation itself.

The $\Sigma^+$ mass was calculated from Eq. (3) by using the following input data:

| | |
|---|---|
| Proton range | $1677.5 \pm 3.2\,\mu$ |
| Proton energy | $18.85 \pm 0.04$ Mev, |
| Proton momentum | $189.01 \pm 0.20$ Mev/c, |
| Proton mass | $938.213 \pm 0.01$ Mev, |
| $\pi^0$ mass | $135.00 \pm 0.05$ Mev. |

The result of the calculation is

$$M_{\Sigma^+} = 1189.33 \pm 0.22 \text{ Mev},$$

and is taken as our best estimate of the $\Sigma^+$ mass.
The Q value for the decay, calculated from Eq. (4), is

$$Q_{\Sigma^+ \to p} = 116.12 \pm 0.22 \text{ Mev}.$$

## 2. The Decay Mode $\Sigma^+ \to n + \pi^+$ at Rest

Twenty-one pions from these decays were followed to rest and their ranges measured. Two of these were in the 2B stack and 19 were in the A stack. In addition, five pions left the A stack with residual ranges less than 5mm as determined by ionization measurements, and presumable were positive pions from decays at rest. These 26 ranges were used to calculate a mean normalized pion range of $92.48 \pm 0.49$ mm. The error is calculated as for the proton range, but with 2.6% Bohr range straggling and 1/2% measurement error. Each range was measured on the automated microscope by two different observers.

The normalized range distribution is shown in Fig. 8. The spread of the distribution is 2.31 mm (2.5%)—slightly less than predicted by straggle alone. The internal and external estimates of the error on the mean range are, respectively, $\pm 0.44$ mm and $\pm 0.49$ mm.

The energy corresponding to the mean range is 91.72±0.44 Mev—the error being compounded from the range error and the assumed 1/2% systematic error in the range-energy relation in this region.   The quantities pertinent to the calculations are:

Pion range        92.48 ± 0.49 mm,

Pion energy       91.72 ± 0.44 Mev,

Pion momentum     184.44 ± 0.55 Mev/c,

Neutron mass      939.506 ± 0.01 Mev.

These data yield

$$M_{\Sigma^+} = 1188.75 \pm 0.54 \text{ Mev},$$

$$Q_{\Sigma^+ \to n} = 115.54 \pm 0.54 \text{ Mev}.$$

This mass value differs from that obtained by using the proton decay mode by 0.58 ± 0.63 Mev.   Although the results are consistent, a small error in the range-energy relation for pions of range about 9 cm may contribute to the difference.

3.   The Mass of the Neutral Particle in the Proton Decay Mode

The mass of the neutral pion can be measured by combining the $\Sigma^+$ mass determined from the mode $\Sigma^+ \to n + \pi^+$ with the proton energy from the proton decay mode according to the equation

$$M^0 = \left[ (M_\Sigma - M_p)^2 - 2M_\Sigma T_p \right]^{1/2} = 134.0 \pm 1.0 \text{ Mev}.$$

This value agrees with the best value, 135.00 ± 0.05 Mev, quoted by Barkas and Rosenfeld.[19]   It is the first direct measurement of the mass of the neutral partner in this decay.

## B. Σ-Hyperon—Lifetime Measurements

The hyperons located in the A stack were used to obtain estimates of the $\Sigma^+$ and $\Sigma^-$ lifetimes. In this stack, all the star prongs of greater than about twice-minimum ionization were followed to their terminations regardless of the characteristics of the parent $K^-$ star; we consider the sample of hyperons thus obtained to be unbiased.

### 1. The Maximum-Likelihood Method

The maximum-likelihood method was used to estimate the lifetimes.[25-28] Two different likelihood functions could be written: one considering only those particles that decayed in flight; and the other considering, in addition, those that came to rest. Typically, hyperons produced by $K^-$ interactions at rest in emulsion have moderation times of the same order as their lifetimes; therefore, either expression can be used to estimate the lifetimes.

The likelihood expression used when only decays in flight are considered is

$$P(r) = \prod_i^{N_F} r \exp(-rt_i)/[1 - \exp(-rT_i)] , \qquad (5)$$

where

r    is the decay rate,

$t_i$   is the flight time for the ith decay,

$T_i$   is the initial moderation time for the ith particle (the

proper time for the particle to come to rest had it not decayed),

$N_F$   is the number of decays.

When decays at rest are also considered, the expression becomes

$$P(r) = \prod_i^{N_F} r \exp(-rt_i) \prod_j^{N_R} \exp(-rT_j) \qquad (6)$$

where

r   is the decay rate,

$t_i$   is the flight time for the _i_th decay in flight,

$T_j$   is the moderation time for the _j_th decay at rest,

and

$N_F$  and  $N_R$  are the numbers of decays in flight and at rest respectively.
In either expression, the most likely decay rate is defined as that value of  r
which makes P(r) a maximum.  The value of the most likely decay rate can be
determined by differentiation, and is

$$\frac{1}{r} = \frac{1}{N_F} \sum_i^{N_F} \left\{ t_i + \left[ T_i / e^{rT_i} - 1 \right] \right\} \tag{7}$$

for decays in flight only, or

$$\frac{1}{r} = \frac{1}{N_F} \left( \sum_i^{N_F} t_i + \sum_j^{N_R} T_j \right) \tag{8}$$

for decays at rest and for decays in flight.

The statistical uncertainty in the value of  r  is estimated by the Bartlett'S
function,

$$S(r) = \frac{\sum_i^{N_F} \left[ rt_i - 1 + \frac{rT_i e^{-rT_i}}{\left( 1 - e^{-rT_i} \right)} \right]}{\left\{ \sum_i^{N_F} \left[ 1 - \frac{r^2 T_i^2 e^{-rT_i}}{\left( 1 - e^{-rT_i} \right)^2} \right] \right\}^{1/2}} \tag{9}$$

when only decays in flight are considered, and by

$$S(r) = \left[\left(\sum_{i}^{N_F} t_i + \sum_{j}^{N_R} T_j\right) - \frac{N_F}{r}\right](N_F)^{-1/2} \tag{10}$$

when decays at rest are included.

## 2. Measurements

The data needed to calculate the decay rates are the times which enter the foregoing equations. Moderation times are obtained from ranges with the aid of the tables of Barkas and Young.[18] For particles that come to rest, the procedure is straightforward. For decays in flight, however, the residual range at the decay point must be determined, and added to the measured range to give the initial potential range, from which the initial moderation time is calculated. The flight time is the difference between the initial moderation time and the residual moderation time at the decay point.

The residual ranges of the decays in flight can be determined in two ways: either from the range and angle of emission of the charged decay product, or from the ionization of the hyperon. We have used both methods. Our procedure was to calculate the hyperon velocity from kinematics, where possible, estimating the error by compounding the errors in secondary range and angle of emission. If the error was comparable to that which would be obtained from ionization measurements, ionization was also used to estimate the hyperon velocity, and the best value was calculated from the two techniques. In practice, the velocities of those hyperons decaying via $\Sigma^+ \rightarrow p + \pi^0$ were obtained almost exclusively from kinematics, but the two techniques were generally comparable for decays via the pion modes.

### 3. The $\Sigma^+$ Lifetime Determined by the Proton Decay Mode

A total of 107 $\Sigma^+$ decays into protons were analyzed to calculate the
$\Sigma^+$ decay rate. Of these, 43 were decays in flight and 64 were decays at rest.
Considerable care was taken to avoid overlooking those decays which simulated
proton scatterings without change in ionization; the scanners were instructed to
consider every "scattering" a possible $\Sigma^+$ decay. Each such event was checked
for compatibility with the decay mode $\Sigma^+ \to p + \pi^0$. The final sample of decays
in flight was checked for observational bias by calculating the decay angles
in the rest system of the hyperon; the distribution of angles was found to be
isotropic and therefore no correction for missed events was considered
necessary.

The results obtained with these data are shown in Fig. 9, where curve 1
represents the total sample of 107 decays and curve 2 represents the 43 decays
in flight. The lifetimes corresponding to the maxima of these curves are

$$\tau^+ = 0.85^{+0.15}_{-0.11} \times 10^{-10} \text{ sec (flight and rest)},$$

$$\tau^+ = 0.86^{+0.75}_{-0.27} \times 10^{-10} \text{ sec (flight only)}.$$

The errors were estimated by using Eqs. (9) and (10). A graph of Eq. (9)
for these data is included in Fig. 10.

### 4. The Hyperon Lifetimes from the Pion Decay Modes

Several difficulties not present in the previous analysis complicate
the determination of the decay rates in the pion modes. Before the data and
results are described, we must mention these considerations: (a) The charge
of the hyperon can be determined only if either the decay pion or the pion

partner is identified, or if the decay occurs at rest. (b) The $\Sigma^-$ interacts
when it comes to rest. (Frequently, however, no star is produced and the event
is not recognized.) (c) The efficiency for detecting decays via the pion mode
is less than 100%, particularly for decays at rest. (d) Ionization measurements
must frequently be relied upon to fix the hyperon velocity at decay. The
residual and flight times are therefore subject to larger errors than in decay
via the proton mode.

The techniques used to overcome these difficulties are elaborated in
the following sections. Two separate analyses are presented, one using only
decays in flight, and the other using also the decays and interactions at rest.

a. The lifetimes from decays in flight.

From a total sample of 94 decays in flight, we identified 26 $\Sigma^-$ hyperons
and 33 $\Sigma^+$ hyperons; the charges of the remaining 35 decays could not be
determined. The data from these events were used to calculate the likelihood
function, Eq. (5). The lifetimes determined from the resulting curves are

$$\tau^+ = 0.63^{+0.48}_{-0.19} \times 10^{-10} \text{ sec} \qquad \text{for } 33 \ \Sigma^+ \to n + \pi^+ \text{ in flight,}$$

$$\tau^- = 1.16^{+1.47}_{-0.43} \times 10^{-10} \text{ sec} \qquad \text{for } 26 \ \Sigma^- \to n + \pi^- \text{ in flight,}$$

$$\tau^\pm = 0.93^{+0.32}_{-0.19} \times 10^{-10} \text{ sec} \qquad \text{for } 94 \ \Sigma^\pm \to n + \pi^\pm \text{ in flight.}$$

The lifetimes above are shorter than the currently accepted values—an effect
that has been observed by other workers in emulsions.[24, 25, 29-37] It appears,
however, that a general displacement toward short lifetimes has occurred—
the mixed lifetime is intermediate between the $\Sigma^+$ and $\Sigma^-$ lifetimes, and the
$\Sigma^-$ lifetime is about twice that of the $\Sigma^+$. It is our belief that the statistical

errors made in the velocity measurements are reflected asymmetrically in
the mean lives. Similar conclusions have been reached by Freden et al.[29]

### b. Lifetime estimates with events at rest included

According to Eq. (6), if the sample of particles whose lifetime is to be
determined includes events at rest, the $T_i$ for the decays in flight do not enter
the calculations. Because the $T_i$ are presumably to blame for the low values
of $\tau$ calculated previously, this second analysis was undertaken. The same
decays in flight are used here as were used previously, but now the values
of $T_i$ are not required.

Because there are decays in flight whose charge is not known, no
complete sample of events can be selected for either the $\Sigma^+$ or $\Sigma^-$ calculation.
Instead, a joint likelihood function must be constructed which includes particles
of both charges and allows for two different lifetimes. Such a function can be
constructed, and is given by

$$P(x,y) = \left[\prod_j^{N_{R^+}} \exp(-xT_j)\right]\left[\prod_k^{N_{R^-}} \exp(-yT_K)\right]\prod_i^{N_F}\left[P_i x\exp(-xt_i)\right.$$

$$\left. + (1-P_i)\, y\, \exp(-yt_i)\right], \qquad (11)$$

where $x$ and $y$ are the $\Sigma^+$ and $\Sigma^-$ decay rates, respectively. The first
product is over the $\Sigma^+$ decays at rest, the second is over the $\Sigma^-$ interactions
at rest, and the third is over the decays in flight; $P_i$ is defined as the probability
that the $i$th decay in flight is a $\Sigma^+$.

Equation (11) can be solved to give the most likely decay rates:

$$\frac{1}{x} = \frac{\sum\limits_{j}^{N_{R^+}} T_j + \sum\limits_{m}^{N_{F^+}} t_m}{N_{F^+}} - \frac{1}{N_{F^+}} \sum\limits_{i}^{N_{F^\pm}} \frac{P_i \exp(-xt_i)(1-xt_i)}{P_i x \exp(\frac{1}{2}xt_i) + (1-P_i)y \exp(-yt_i)} \ .$$

$$\tag{12}$$

$$\frac{1}{y} = \frac{\sum\limits_{k}^{N_{R^-}} T_k + \sum\limits_{n}^{N_{F^-}} t_n}{N_{F^-}} - \frac{1}{N_{F^-}} \sum\limits_{i}^{N_{F^\pm}} \frac{(1-P_i)\exp(-yt_i)(1-yt_i)}{P_i x \exp(-xt_i) + (1-P_i)y \exp(-yt_i)} \ ,$$

$$\tag{13}$$

where $N_{F^+}$ and $N_{F^-}$ are the numbers of decays in flight of known charge, and $N_{F^\pm}$ is the number of unknown charge. For $N_{F^\pm} = 0$, the two equations are independent.

Before Eqs. (12) and (13) could be used, the $P_i$ and total moderation times had to be calculated. The $P_i$ are estimated by a study of the hyperons of known charge. We find[5]

$P_i = 0.27$ if the $\Sigma$ has energy $> 60$ Mev, has no pion partner, and is

accompanied by a proton of energy $> 30$ Mev from the $K^-$ star;

$P_i = 0.79$ if the $\Sigma$ is as above but without a proton of energy $> 30$ Mev;

$P_i = 1.0$ if the $\Sigma$ has energy $> 60$ Mev and there is no other star prong;

$P_i = 0.62$ if the $\Sigma$ has energy $< 60$ Mev and there is no $\pi$ partner.

There were no decays of unknown charge accompanied by a $\pi$ partner.

The total moderation time for the $\Sigma^-$ interactions at rest must be estimated from the moderation time of those hyperons which produce recognizable stars when they interact. The fraction of those which do so must in turn be estimated from a study of $\Sigma^-$ produced by $K^-$ reactions with free protons, or "collinear events." By combining our data with those reported by the $K^-$ collaboration experiment,[38] a sample of 95 $\Sigma^-$ endings from collinear events is obtained. If we consider as "recognizable" a $\Sigma^-$ star which has more than one prong or which has one prong of $> 200\ \mu$ range, then we find that there are 30 recognizable stars among the 95 $\Sigma^-$ endings. The ratio of all $\Sigma^-$ endings to recognizable $\Sigma^-$ endings is, therefore, $95/30 = 3.17 \pm 0.48$.

In the A stack, there are 40 star prongs which terminate at rest with the production of a recognizable star, and appear to be $\Sigma^-$ hyperons. To check this identification, the $\pi$ partners were followed when they existed. Only 18 of the these $K^-$ stars produced a $\pi$ partner, 15 of which were identified as $\pi^+$ mesons; the remaining three could not be identified. No $\pi^-$ partner that would signal a hyperfragment rather than a $\Sigma^-$ was found.

The total $\Sigma^+$ moderation time was obtained from the ranges of 51 observed $\Sigma^+ \to \pi^+ + n$ decays at rest, plus a small correction for the observational loss of such decays. This correction was estimated by studying the distribution of decays as a function of depth in emulsion, and also by studying the distribution of dip angles of the emitted pions. We estimate that four $\Sigma^+ \to \pi^+ + n$ decays at rest escaped detection.

5. Final Calculation of the Lifetime

Equations (12) and (13) were solved on an IBM 650 computer using the best estimates for the quantities involved, as outlined previously. The most likely lifetimes were found to be $\tau^+ = 0.80 \times 10^{-10}$ sec and $\tau^- = 1.75 \times 10^{-10}$ sec.

The errors introduced into these values by errors in the input data were determined as follows:

(a) The effect of uncertainties in the total moderation times was calculated directly by altering these times by one standard deviation, then recalculating the lifetimes.

(b) The sensitivity to changes in the $P_i$ was estimated by setting all $P_i$ equal to 0.5 and again recalculating the lifetimes.

The statististical errors were estimated by plotting Eq. (11), first as a function of x, with y fixed at its most likely value, and then as a function of y, with x fixed. These curves are shown in Fig. 11. The spread of the curves at 60% height was taken as the statistical uncertainty. The same result was obtained from Eq. (12) when the total number of $\Sigma^+$ and $\Sigma^-$ decays in the unknown group was estimated from the $P_i$.

The uncertainties introduced are listed below:

| Error | $\Delta \tau^+ \times 10^{-10}$ sec | $\Delta \tau^- \times 10^{-10}$ sec |
|---|---|---|
| $\Sigma^-$ moderation time | ± 0.005 | ± 0.19 |
| $\Sigma^+$ moderation time | ± 0.02 | negligible |
| $P_i$ | 0.02 | 0.02 |
| Statistical | +0.13, -0.10 | +0.34, -0.24 |

The best estimates of the lifetimes, from the pion decay modes, are

$$\tau^+ = 0.80^{+0.14}_{-0.11} \times 10^{-10} \text{ sec,}$$

$$\tau^- = 1.75^{+0.39}_{-0.30} \times 10^{-10} \text{ sec.}$$

By combining this value for $\tau^+$ with our value obtained from the proton decay mode, we have

$$\tau^+ = 0.82^{+0.10}_{-0.08} \times 10^{-10} \text{ sec}$$

as our best estimate of the $\Sigma^+$ lifetime.

These values are in good agreement with other published values from emulsions and bubble chambers.[19] Further, the lifetime of the $\Sigma^+$ is the same when calculated from either the pion or proton decay mode of this particle if events at rest are included. This is strong evidence that the low values obtained for decays in flight via the pion modes result from experimental biases and that it is not necessary to introduce an unknown particle of short lifetime to explain the result.

## C. Branching Ratios

### 1. The Branching Ratio $(\Sigma^+ \to p + \pi^0)$ / all $\Sigma^+$

As mentioned before, 107 $\Sigma^+$ decays into protons have been observed in the A stack, and the efficiency in detecting these has been taken to be 100%. The total number of $\Sigma^+$ decays into $\pi^+$ mesons can now be calculated as follows:

(a) There are 51 decays at rest and 33 decays in flight known to be $\Sigma^+ \to n + \pi^+$.

(b) There are 35 decays in flight into pions of unknown charge. The number of $\Sigma^+ \to n + \pi^+$ represented by this group is estimated to be $\Sigma P_i = 17$.

(c) It has been estimated that four decays at rest were lost by failure to observe the pion.

By combining these numbers, we find that the total number of $\Sigma^+ \to n + \pi^+$ is 105.

The branching ratio therefore is

$$\frac{\Sigma^+ \to p + \pi^0}{\text{all } \Sigma^+ \text{ decays}} = \frac{107}{212} = 0.50 \pm 0.03 \,,$$

which agrees with recent values from bubble chamber and emulsion groups.[29,39]

### 2. The Branching Ratio $(\Sigma^+ \to p + \gamma)/(\Sigma^+ \to p + \pi^0)$

The decay mode $\Sigma^+ \to p + \gamma$ occurring at rest would produce a proton of 26.5 Mev energy and 3.0 mm range in emulsion. There is no such candidate among the 95 decays at rest via the proton mode in the A, 2B, and 1U stacks. There is, however, the possibility of confusing such a decay with a decay by the normal proton mode occurring slightly in flight; for example, a $\Sigma^+$ with 100 $\mu$ residual range will emit a proton of 3.0 mm range if the decay angle is approximately 50 deg. An event such as this would be classed "in flight" on the basis of the proton range, even though it might not be clear from the hyperon track itself

that the decay did not occur at rest. To check this possibility, the proton ranges from the $\Sigma^+ \to p$ decays in flight in the A and 2B stacks have been plotted in Fig. 12. There is no evidence of grouping around 3 mm, but there are two ranges very close to the expected value from $\Sigma^+ \to p + \gamma$. The actual measured ranges are 3043 $\mu$ and 3047 $\mu$. Neither one of these represents a possible case of $\Sigma^+ \to p + \gamma$ decay, however; in one case the hyperon residual range at the decay point is 2.2 mm, and in the other case it is 1.3 mm. Ionization measurements and kinematic analysis on the assumption that the decays are via the normal proton mode give consistent results. Since these are the only two cases whose proton range is within straggling errors of 3 mm, it is concluded that there are no $\Sigma^+ \to p + \gamma$ decays at rest erroneously classed as $\Sigma^+ \to p + \pi^0$ decays in flight.

An upper limit can be put on the branching ratio on the basis of the 95 decays at rest:

$$\frac{\Sigma^+ \to p + \gamma}{\Sigma^+ \to p + \pi^0} = \frac{0}{95} \text{ observed.}$$

Two other groups have observed a total of zero $\Sigma \to p + \gamma$ decays among 138 $\Sigma^+ \to p + \pi^0$ decays.[29,40] Quareni et al., however, have reported three possible $\Sigma^+ \to p + \gamma$ decays, and estimate the branching ratio to be approx 1%.[41]

Theoretical predictions for this branching ratio range from 0.01% to 1.0%.[42,43]

### 3.  The Branching Ratios for Leptonic Decay

A theoretical prediction based on the assumption of a universal Fermi interaction was that a few percent of all hyperon decays should be via leptonic modes.  The following relevant data were gathered by us in the course of this work:

$$\frac{\Sigma^+ \rightarrow \text{leptons}}{\Sigma^+ \rightarrow \pi^+} = \frac{0}{129} \, ,$$

$$\frac{\Sigma^- \rightarrow \text{leptons}}{\Sigma^- \rightarrow \pi^-} = \frac{0}{67} \, .$$

These ratios alone are sufficient to weaken the above theory, but in the meantime, much more data have been accumulated, particularly by bubble chambers, confirming that experimentally the ratios are smaller than expected.

### D.  Decay Asymmetry

We have looked for an up-down asymmetry in the $\Sigma$-hyperon decay with respect to the $\Sigma\pi$ production plane.  None was found.

For the study we used only two-pronged events of the type $K^- + (p) \rightarrow \Sigma^{\pm} + \pi^{\mp}$, where the $K^-$ meson had come to rest.

We analyzed 181 stars of this kind.  In 94 the $\Sigma$ decay was $\Sigma^{\pm} \rightarrow \pi^{\pm} + n^0$ and in 87 the decay was $\Sigma^+ \rightarrow p + \pi^0$.

We defined the unit vector normal to the "production plane" as $(p_\Sigma \times p_\pi) / \left| p_\Sigma \times p_\pi \right|$ and calculated the cosine of the angle between this normal and the direction of the $\Sigma$-decay secondary.

The up-down asymmetry is defined as $N_+ - N_-/N_+ + N_-$ where $N_+$ = number of events with plus cosine and $N_-$ = number of events with minus cosine.  Further, we defined an asymmetry index, $a$, in the distribution function

$(1 + a \cos \phi)$.  A calculation to find the maximum-likelihood value of a
was made using the actual values of the cosines.  The results of our calculations
of the up-down asymmetries and the most likely values of the asymmetry index
are shown in the table

| Type of decay | $N_+ - N_-/N_+ + N_-$ | a |
|---|---|---|
| $\Sigma^+ \to p + \pi^0$ | $-1/87$ | $-0.02 \pm 0.15$ |
| $\Sigma^+ \to \pi^+ + n^0$ | $4/50$ | $0.19^{+0.19}_{-0.22}$ |
| $\Sigma^\pm \to \pi^\pm + n^0$ | $-6/44$ | $-0.23 \pm 0.22$ |

Thus, no asymmetry is indicated—for either $\Sigma$ decay mode—in the events
we analyzed.

Because our observations were made on reactions in complex nuclei,
in many cases the scattering inside the nucleus may have been sufficient to
cause $(p_\Sigma \times p_\pi)_{observed}$ to be opposite to $(p_\Sigma \times p_\pi)$ at production.  This would
have tended to mask any effect that might have been present.

## ACKNOWLEDGMENTS

# REFERENCES

*This work was done under the auspices of the U. S. Atomic Energy Commission.

†Now at U. S. Naval Postgraduate School, Monterey, California.

‡Now at University of Michigan Radiation Laboratory, Ann Arbor, Michigan.

1.  W. H. Barkas, W. F. Dudziak, P. C. Giles, H. H. Heckman, F. W. Inman, C. J.
    Mason, N. A. Nickols, and F. M. Smith, Phys. Rev. 105, 1417 (1957).

2.  N. Horwitz, J. J. Murray, R. R. Ross, and R. D. Tripp, 450-Mev/c
    $K^--\bar p$ Beams at the Northwest Target Area of the Bevatron Separated
    by the Coaxial Velocity Spectrometer, University of California Radiation
    Laboratory Report UCRL-8269, June 1958 (unpublished).  Also, J. N.
    Dyer, Analysis of the Bevatron $K^-$ Beam by Means of an Emulsion Stack,
    University of California Radiation Laboratory Report UCRL-9364, July
    1958 (unpublished); and Analysis of the Bevatron $K^-$ Beam Transmitted
    by the Murray Spectrometer, University of California, Radiation
    Laboratory Report UCRL-8364 Suppl., January 1959 (unpublished).

3.  H. H. Heckman, F. W. Inman, C. J. Mason, N. A. Nickols, F. M. Smith,
    W. H. Barkas, W. F. Dudziak, and P. C. Giles, Enriched K-Meson
    Beams from the Bevatron, University of California Radiation Laboratory
    Report UCRL-3549, October 1956 (unpublished).

4.  Conrad J. Mason, The Λ-Hyperon Mass and Energy Spectrum from the
    Nuclear Capture of Negative K Mesons (Ph. D. Thesis), Lawrence Radiation
    Laboratory Report UCRL-9297, July 7, 1960 (unpublished).

5.  John N. Dyer, Charged $\Sigma$-Hyperon Production and Decay: Energetics, Lifetimes, and Branching Ratios (Ph. D. Thesis), Lawrence Radiation Laboratory Report UCRL-9450, November 1, 1960 (unpublished).

6.  W. H. Barkas, in Photographie Corpusculaire II ed. by Pierre Demers (University of Montreal Press, 1959), p. 325.

7.  W. H. Barkas, New Facilities and Automatic Track Analysis Equipment at the Lawrence Radiation Laboratory, Lawrence Radiation Laboratory Report UCRL-9180, June 1960 (unpublished).

8.  Norris A. Nickols, The Lifetime and Decay Modes of Negative K Mesons (Ph. D. Thesis), Lawrence Radiation Laboratory Report UCRL-8692, September 1959 (unpublished).

9.  W. H. Barkas, P. H. Barrett, P. Cüer, H. H. Heckman, F. M. Smith, and H. K. Ticho, Nuovo cimento 8, 185 (1958).

10. W. H. Barkas, F. M. Smith, and W. Birnbaum, Phys. Rev. 98, 605 (1955).

11. W. H. Barkas, Nuovo cimento 8, 201 (1958).

12. R. W. Birge, D. H. Perkins, J. R. Peterson, D. H. Stork, M. N. Whitehead, Nuovo cimento 4, 834 (1956).

13. G. Alexander, R. H. W. Johnson, and C. O'Ceallaigh, Nuovo cimento 6, 478 (1957).

14. M. L. T. Kannangara and G. S. Shrikantia, Phil. Mag. 44, 1091 (1953).

15. Y. Eisenberg, W. Koch, E. Lohrmann, M. Nikolic, M. Schneeberger, and H. Winzeler, Nuovo cimento 9, 745 (1958).

16. Y. Eisenberg, W. Koch, E. Lohrmann, M. Nikolic, M. Schneeberger, and H. Winzeler, Nuovo cimento 8, 663 (1958).

17. S. Nilsson and A. Frisk, Arkiv Fysik 14, 293 (1958).

18. W. H. Barkas and D. M. Young, Emulsion Tables: I. Heavy-Particle Functions, Lawrence Radiation Laboratory Report UCRL-2579 (rev) September 1954 (unpublished).

19. W. H. Barkas and A. H. Rosenfeld, Data for Elementary-Particle Physics, Lawrence Radiation Laboratory Report UCRL-8030-Rev., revised 1961 (unpublished).

20. H. C. Burrowes, D. O. Caldwell, D. H. Frisch, D. A. Hill, D. M. Ritson, and R. A. Schluter, Phys. Rev. Letters $\underline{2}$, 117 (1959).

21. G. Lüders and B. Zumino, Phys. Rev. $\underline{106}$, 385 (1957).

22. A. Pais, Phys. Rev. Letters $\underline{3}$, 242 (1959).

23. W. K. H. Panofsky and M. Phillips, Classical Electricity and Magnetism (Addison-Wesley Publishing Company Inc., Redding, Mass, 1955), p. 305.

24. D. Evans, F. Hassan, K. K. Nagpaul, D. J. J. Prowse, M. Rene, G. Alexander, R. H. W. Johnston, D. Keefe, D. H. Davis, W. B. Lasich, M. A. Shaukat, F. R. Stannard, A. Bonetti, C. Dilworth, M. Merlin, and A. Salandin, (K* Collaboration, Part III), Nuovo cimento $\underline{15}$, 873 (1960).

25. M. F. Kaplon, A. C. Melissinos, and T. Yamanouchi, Ann. Phys. $\underline{9}$, 139 (1960).

26. M. S. Bartlett, Phil. Mag. $\underline{44}$, 249 (1953).

27. E. Amaldi, Nuovo cimento $\underline{2}$, (Suppl.) 253 (1955).

28. C. Franzinetti and G. Marpurgo, Nuovo cimento $\underline{6}$, (Suppl.) 577 (1957).

29. S. C. Freden, H. N. Kornblum, and R. S. White, Nuovo cimento $\underline{4}$, 611 (1960).

30. D. A. Glaser, M. L. Good, and D. R. O. Morrison, in Proceedings of
    the 1958 Annual International Conference on High-Energy Physics
    at Cern (CERN, Geneva, 1958), p. 270.

31. G. A. Snow, in Proceedings of the Seventh Annual Rochester Conference
    on High-Energy Nuclear Physics (Interscience Publishers, Inc.,
    New York, 1957), p. viii-14.

32. R. G. Glasser, N. Seeman, and G. A. Snow, Phys. Rev. 107, 277 (1957).

33. J. H. Davies, D. Evans, P. H. Fowler, R. R. François, M. W. Friedlander,
    R. Hiller, P. Iredale, D. Keefe, M. G. K. Menon, D. H. Perkins, and
    C. F. Powell, Nuovo cimento 4, (Suppl.) 472 (1956).

34. W. F. Fry, J. Schneps, G. A. Snow, M. S. Swami, and D. C. Wold,
    Phys. Rev. 107, 257 (1957).

35. S. C. Freden, F. C. Gilbert, and R. S. White, Bull. Am. Phys. Soc. 3,
    25 (1958).

36. W. Koch, M. Nikolic, M. Schneeberger, and H. Winzeler, Helv. Phys.
    Acta 32, 549 (1959).

37. D. A. Glaser (Lawrence Radiation Laboratory, Berkeley), Data Collected
    for the 1959 Kiev Conference on High-Energy Physics (Unpublished).

38. B. Bhowmik, D. Evans, D. Falla, F. Hassan, A. A. Kamal, K. K. Nagpaul,
    D. J. Prowse, M. René, G. Alexander, R. H. W. Johnston, C. O'Ceallaigh,
    D. Keefe, E. H. S. Burhop, D. H. Davis, R. C. Kumar, W. B. Lasich,
    M. A. Shaukat, F. R. Stannard, M. Bacchella, A. Bonetti, C. Dilworth,
    G. Occhialini, L. Scarsi, M. Grilli, L. Guerriero, L. von Lindern,
    M. Merlin, and A. Salandin, (K$^-$ Collaboration, Part II), Nuovo
    cimento 14, 315 (1959).

39. J. Leitner, P. Nordin, Jr., A. H. Rosenfeld, F. T. Solmitz, and
    R. D. Tripp, Phys. Rev. Letters $\underline{3}$, 186 (1959).

40. R. G. Glasser, N. Seeman, and G. A. Snow, NRL Quarterly on Nuclear
    Science (April 1960).

41. G. Quareni, A. Quareni Vignudelli, G. Dascolo, and S. Mora,
    Nuovo cimento $\underline{14}$, 1179 (1959).

42. R. F. Behrends, Phys. Rev. $\underline{111}$, 1691 (1958).

43. P. Prakash and A. H. Zimerman, Nuovo cimento $\underline{11}$, 869 (1950).
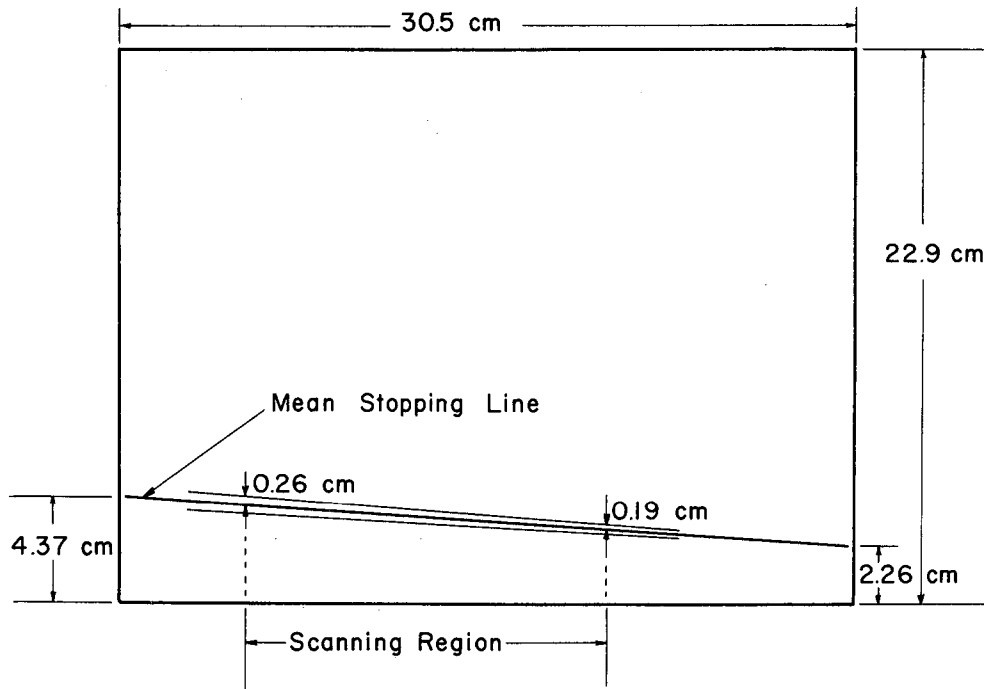
Fig. 1.  Diagram indicating stopping positions for K⁻ mesons in pellicles of the  2B  stack.
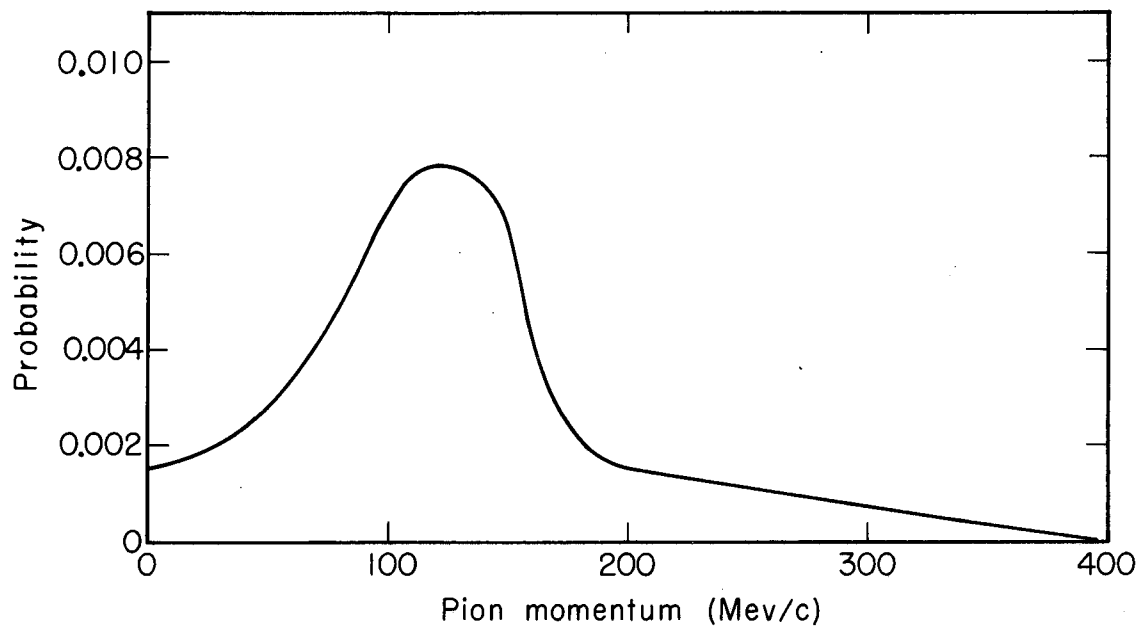
Fig. 2.  Assumed spectrum of $\pi^-$ from $K^-$ interactions in flight.
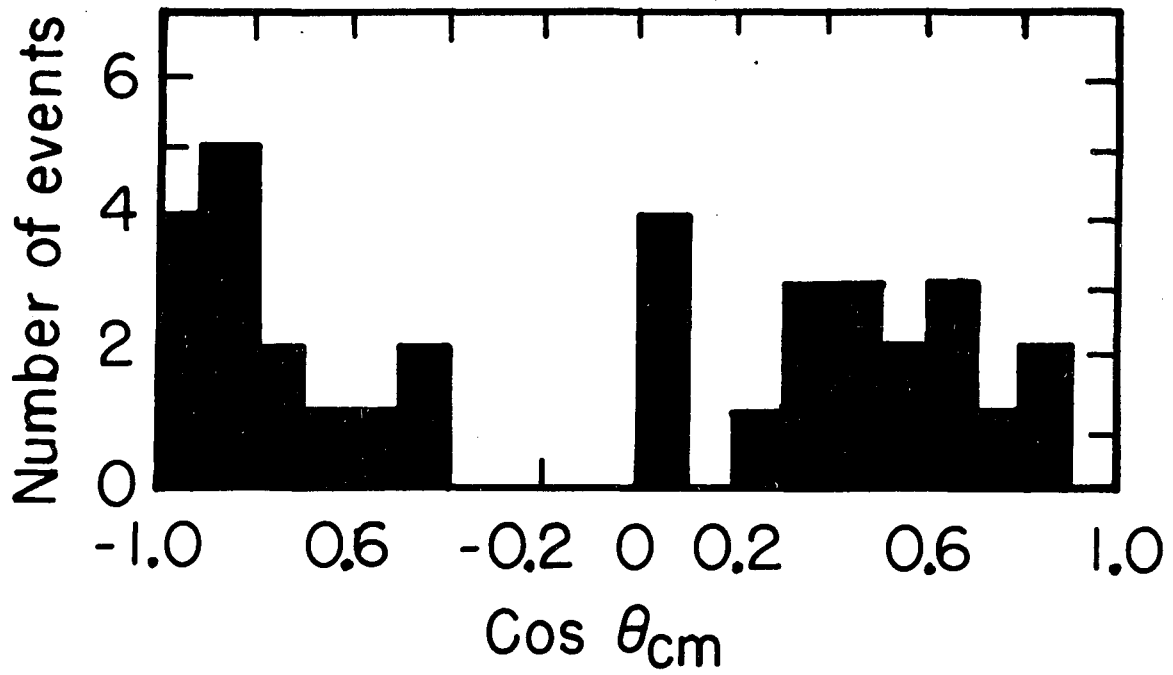
Fig. 3.   Cosine of c. m. angle for two-body decays.
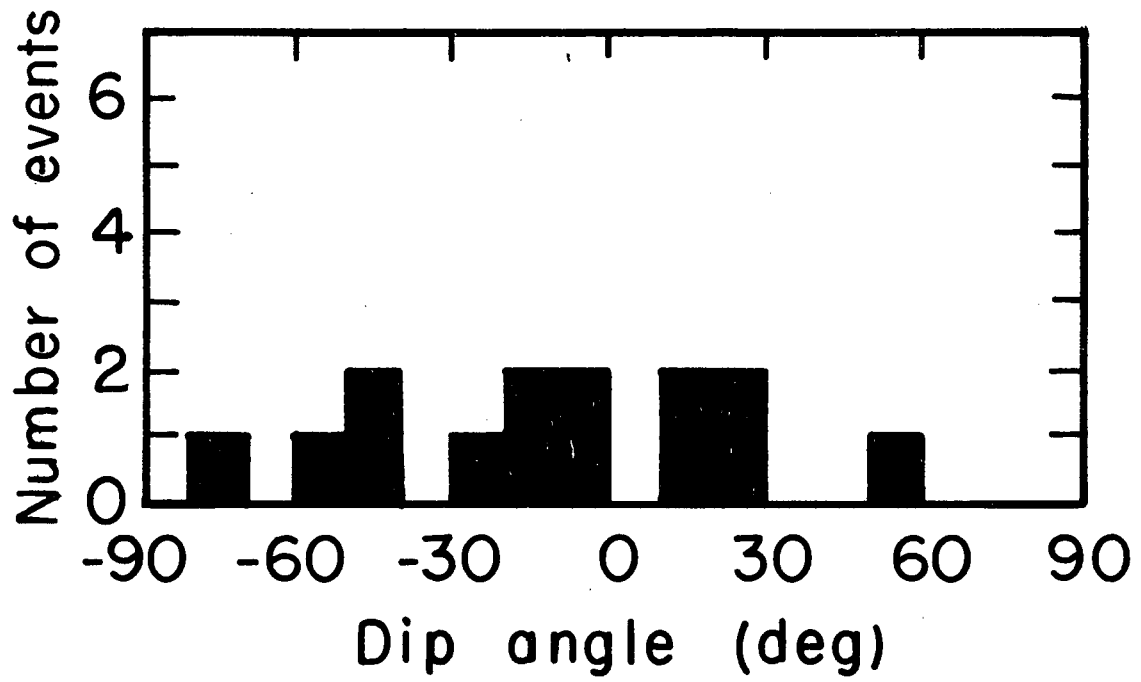
MU-23887

MU-23888

Fig. 4.   Dip angle of equatorial two-body decays.
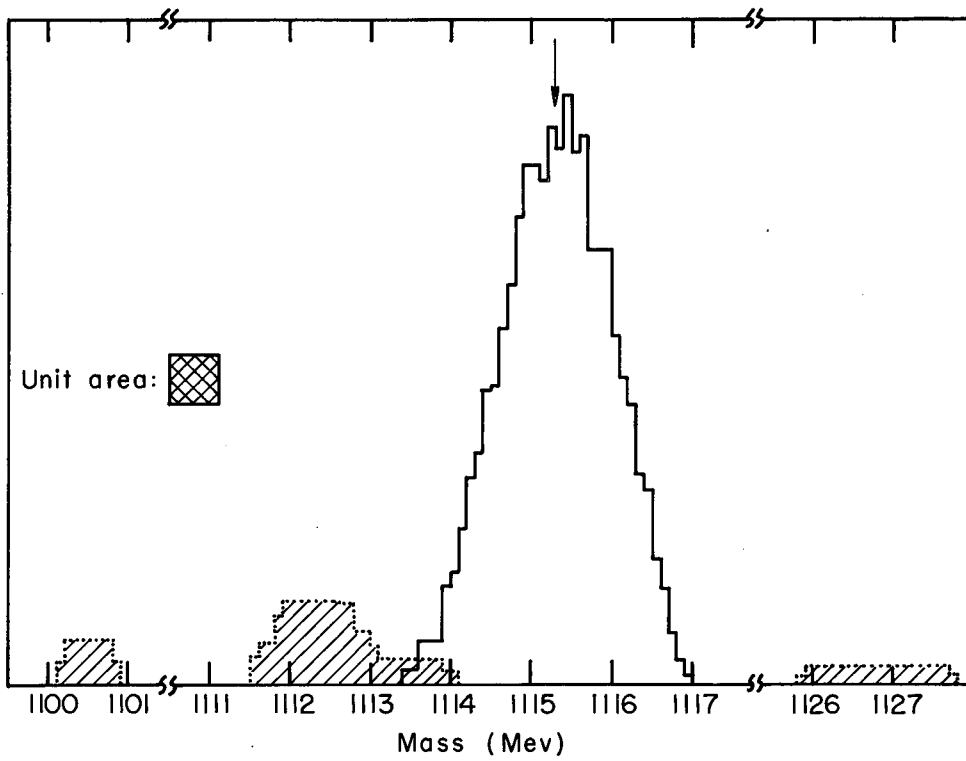
Fig. 5.  Mass value ideogram for the  2B  stack.  The mean
         value, indicated by the arrow, is 1115.26 Mev;  the
         statistical error in this result is ± 0.11 Mev (29 events).
         Shaded areas correspond to background events.
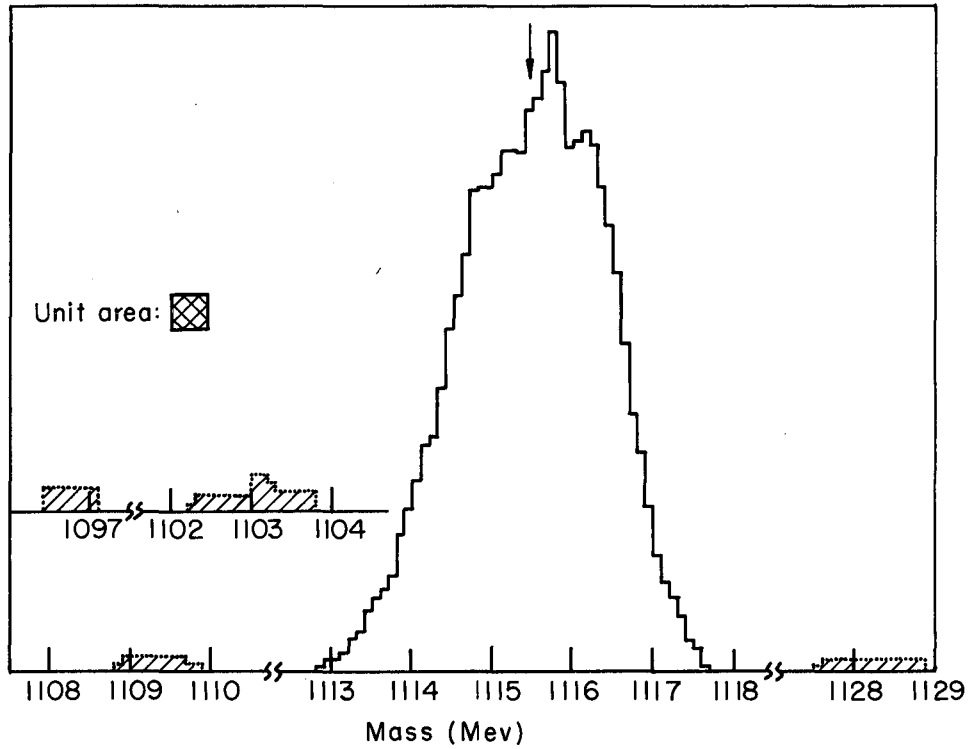
Fig. 6.   Mass value ideogram for the  2D stack.   The mean
value, indicated by the arrow, is 1115.42 Mev;  the
statistical error in this result is ± 0.08 Mev (87 events).
Shaded areas correspond to background events.
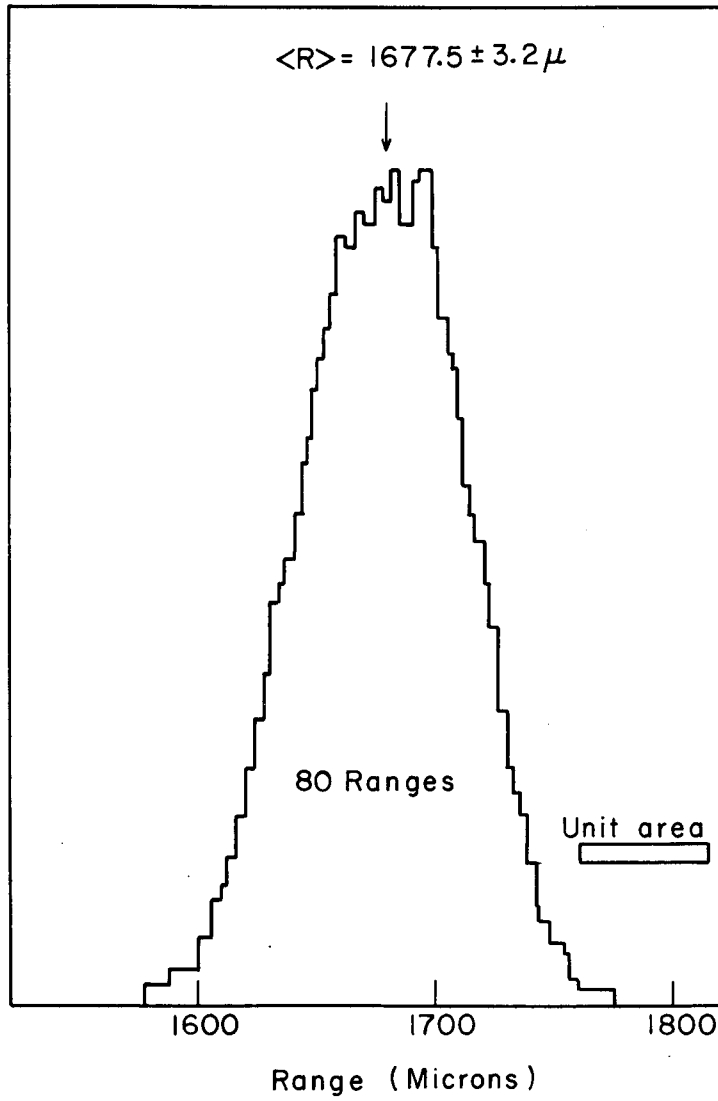
Fig. 7. Proton range ideogram for 80 protons from $\Sigma^+ \longrightarrow p + \pi^0$ decays at rest in the A, 2B, and 1U stacks.
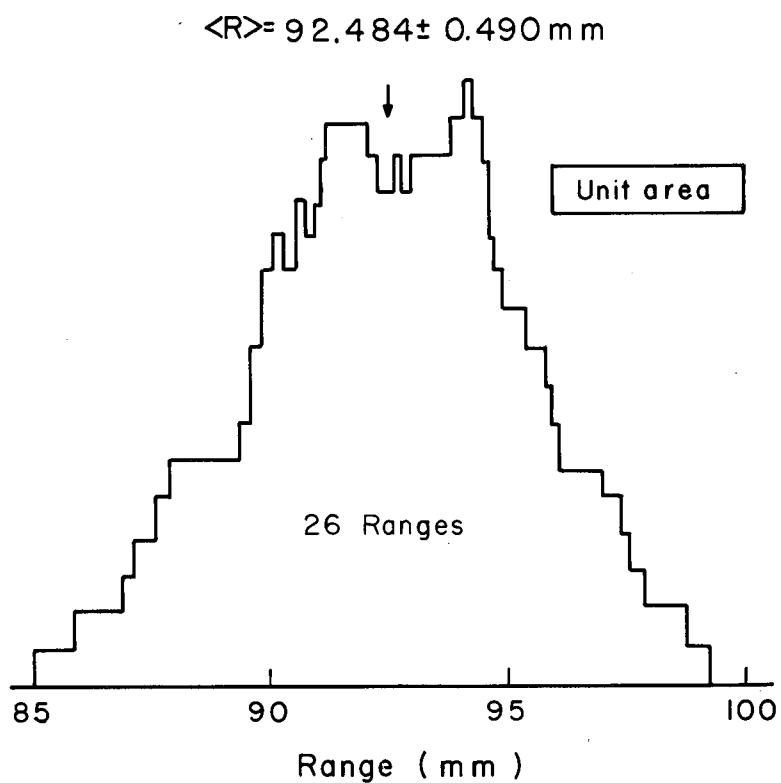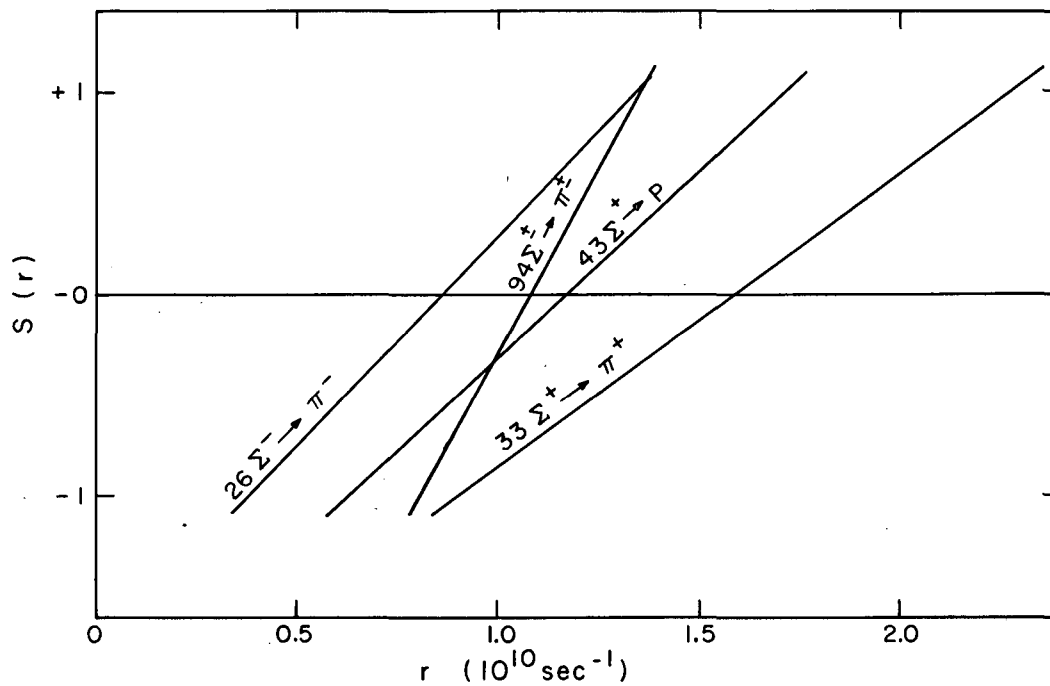
Fig. 8.   Pion range ideogram for 26 pions from $\Sigma^+ \rightarrow n + \pi^+$ decays at rest.   All but two of the events are in the  A stack.
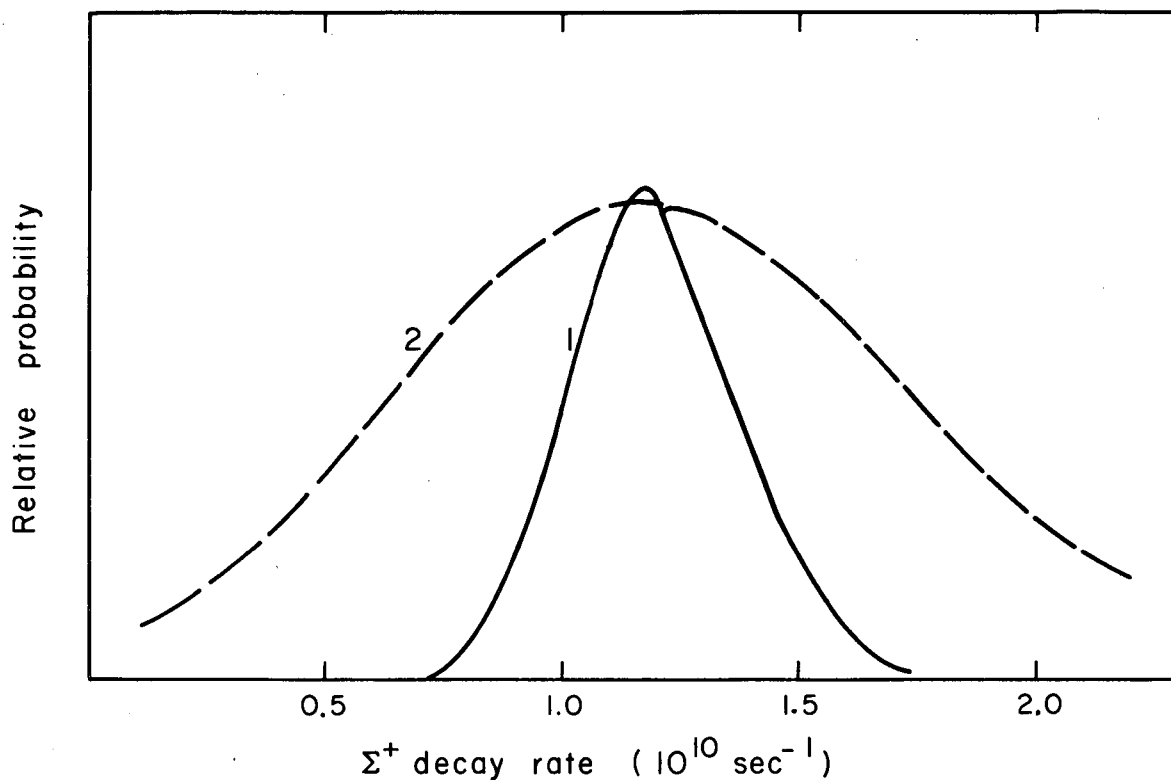
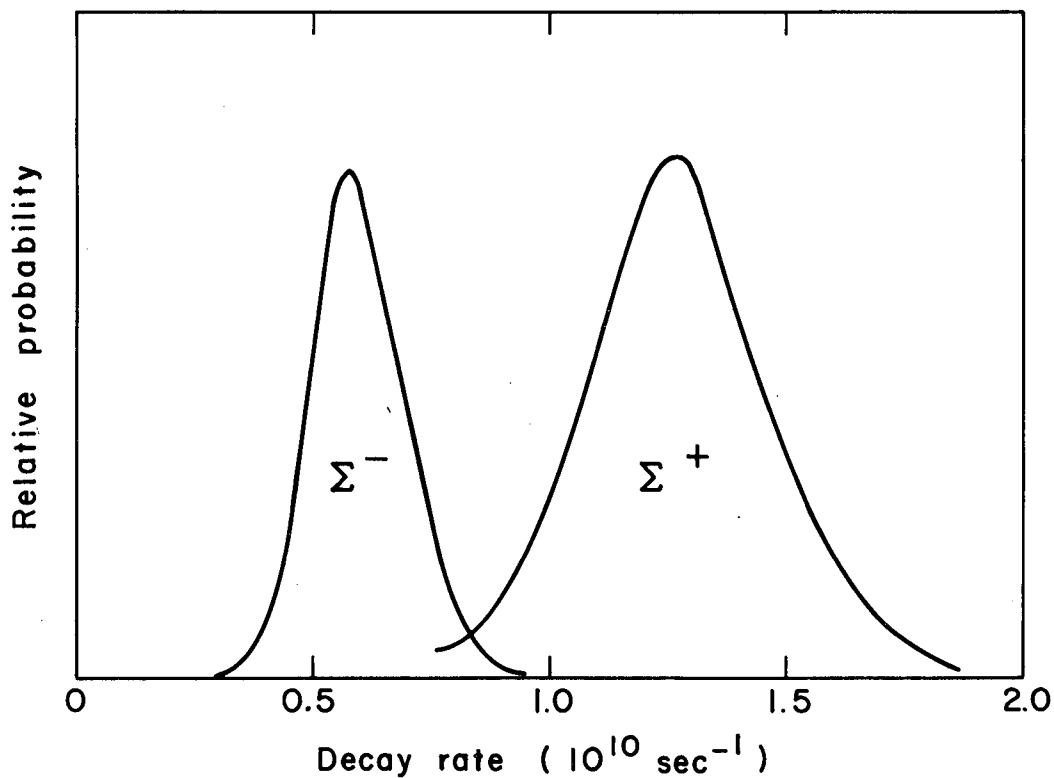Fig. 9. The relative likelihood function versus the decay
rate for $\Sigma^+$ decays via the proton mode: (1) 64 decays
at rest and 43 decays in flight, (2) 43 decays in flight
only.

Fig. 10.  Plot of S(r) versus r, the decay rate.  The values
       of  r  for which S(r) is 0 give the most likely rates,  and the
       values of  r  for which S(r) = ± 1.0 indicate the statistical
       uncertainty in the most likely rate.

Fig. 11.   The joint likelihood function versus the decay rate.
The curve for $\Sigma^-$ is plotted with the $\Sigma^+$ decay rate
held constant at its most likely value, and vice versa.

MU-22069
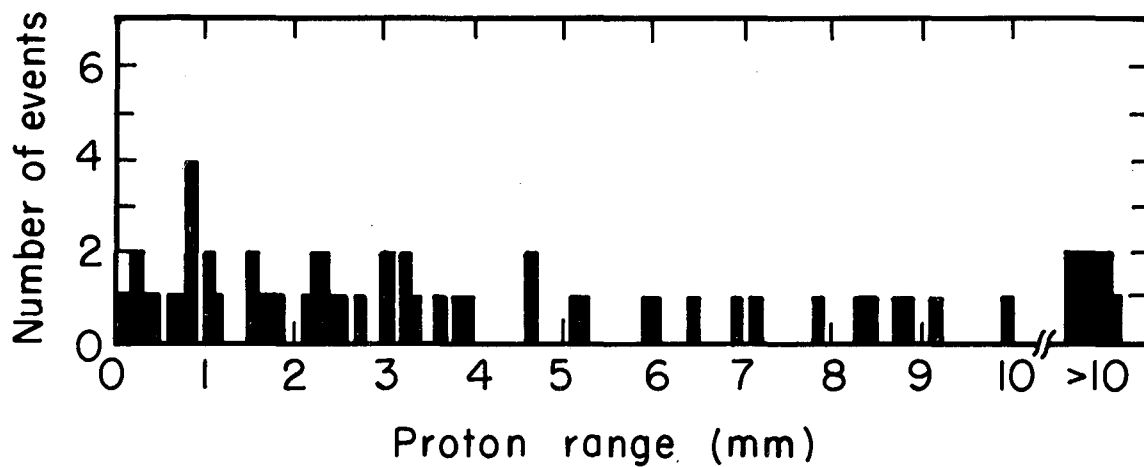
Fig. 12.  Proton ranges from  $\Sigma^+ \longrightarrow p + \pi^0$  decays in flight in the A and 2B stacks.

MU – 23890